JB Journals.ASM.org

Characterization of the *phd-doc* and *ccd* Toxin-Antitoxin Cassettes from *Vibrio* Superintegrons

Anne-Marie Guérout,[a,b] Naeem Iqbal,[a,b]* Natacha Mine,[c] Magaly Ducos-Galand,[a,b] Laurence Van Melderen,[a] Didier Mazel[a,b]

Institut Pasteur, Unité Plasticité du Génome Bactérien, Département Génomes et Génétique, Paris, France[a]; CNRS, UMR 3525, Paris, France[b]; Laboratoire de Génétique et Physiologie bactériennes, Institut de Biologie et Médecine Moléculaires, Faculté des Sciences, Université Libre de Bruxelles, Gosselies, Belgium[c]

Toxin-antitoxin (TA) systems have been reported in the genomes of most bacterial species, and their role when located on the chromosome is still debated. TA systems are particularly abundant in the massive cassette arrays associated with chromosomal superintegrons (SI). Here, we describe the characterization of two superintegron cassettes encoding putative TA systems. The first is the *phd-doc*$_{SI}$ system identified in *Vibrio cholerae* N16961. We determined its distribution in 36 *V. cholerae* strains and among five *V. metschnikovii* strains. We show that this cassette, which is in position 72 of the *V. cholerae* N16961 cassette array, is functional, carries its own promoter, and is expressed from this location. Interestingly, the *phd-doc*$_{SI}$ system is unable to control its own expression, most likely due to the absence of any DNA-binding domain on the antitoxin. In addition, this SI system is able to cross talk with the canonical P1 phage system. The second cassette that we characterized is the *ccd*$_{Vfi}$ cassette found in the *V. fischeri* superintegron. We demonstrate that CcdB$_{Vfi}$ targets DNA-gyrase, as the canonical CcB$_F$ toxin, and that *ccd*$_{Vfi}$ regulates its expression in a fashion similar to the *ccd*$_F$ operon of the conjugative plasmid F. We also establish that this cassette is functional and expressed in its chromosomal context in *V. fischeri* CIP 103206T. We tested its functional interactions with the *ccdAB*$_F$ system and found that CcdA$_{Vfi}$ is specific for its associated CcdB$_{Vfi}$ and cannot prevent CcdB$_F$ toxicity. Based on these results, we discuss the possible biological functions of these TA systems in superintegrons.

Toxin-antitoxin (TA) systems were originally discovered on low-copy-number plasmids through the stabilizing role that they play in these replicons (for recent reviews on TA systems, see references 1, 2, and 3). They are generally composed of two genes encoding a toxin and an antitoxin that antagonizes the toxin activity or prevents its synthesis. The antitoxin can be either an RNA (type I and III systems [4]) or a protein (type II systems), while the toxin is always a protein. In type II systems, the antitoxin and toxin genes are organized in operons whose expression is generally autoregulated at the transcriptional level by the toxin-antitoxin complex. The antitoxin is unstable and degraded by ATP-dependent proteases. The toxin is stable and inhibits an essential cellular process (e.g., replication, translation, or peptidoglycan synthesis). These type II systems have more recently been identified as genuine components of the chromosome of most bacteria (5–7), with up to more than 80 predicted TA systems in the *Mycobacterium tuberculosis* genome (8). Although their stabilization capacity is clearly established when they are located on plasmids, their role when located on the chromosome is much less evident and is still debated (2). There are currently as many as six proposed nonexclusive hypotheses regarding the biological roles of these chromosomal elements (2). The first four roles can be described as physiological or developmental regulators. TA systems were proposed to be in charge of a programmed cell death-like response, allowing altruistic suicide under stressful conditions (reviewed in reference 9). However, this hypothesis is controversial, as several groups failed to reproduce the original observations (see reference 10). A second proposed role, substantiated by the work of Gerdes and colleagues, is that TA systems could act as growth modulators involved in cell survival under unfavorable conditions (11). In relation to a role for survival, TA systems have also been proposed to be involved in the production of persister cells within bacterial populations (12). Persisters consist of a small fraction of cells that are in a dormant state and appear to be resistant to stress conditions, such as antibiotic treatments (for a review, see reference 13). TA systems have also been proposed to play a role of development regulators in *Myxococcus xanthus* (14). The last two hypothetical roles proposed for chromosomal TA are more in line with their original function in plasmids. First, it has been shown that these systems could protect their host genome from colonization by an incoming mobile element or a plasmid carrying a TA from the same functional family by allowing its harmless loss through neutralization of the toxin of the invading element by the chromosomal antitoxin (15, 16). Also, they have been proposed to stabilize chromosomal regions by preventing accidental deletions, especially when located in unstable segments such as mobile genetic elements (MGE) (17–19), as, for example, in integrative and conjugative elements such as SXT (19, 20). In this line, it is striking to notice that TA systems are extremely common in cassettes of chromosomal integrons, especially in superintegrons (SI), (for a review, see reference 21).

Superintegrons gather hundreds of cassettes in *Vibrio* genomes (17, 22), mostly of unknown functions. Cassettes are in most cases promoterless and are thought to constitute a silent reservoir of adaptive functions (17, 23). Silent cassettes can be called on for expression through recombination to an expression spot, in most

Received 1 August 2012 Accepted 3 March 2013
Published ahead of print 8 March 2013
Address correspondence to Didier Mazel, mazel@pasteur.fr.
* Present address: Naeem Iqbal, Centre de recherche en infectiologie, Centre Hospitalier Universitaire de Québec, Québec, Canada.
Supplemental material for this article may be found at http://dx.doi.org/10.1128/JB.01389-12.

doi:10.1128/JB.01389-12

TABLE 1 *Escherichia coli* strains used in this study

Strain	Genotype or description	Reference or source
DH5α	*supE44* Δ*lacU169*(ϕ80d*lacZ*ΔM15) Δ*argF hsdR17 recA1 endA1 gyrA96 thi-1 relA1*	Laboratory collection
β2163	MG1655::Δ*dap*::(*erm pir*)*RP4-2*Tc::*Mu* (Km)	76
MC1061	F$^-$ *araD139* Δ(*araA-leu*)7697 Δ(*ccdB-lacI*)*3 galK16 galE15 hsdR2 relA1 spoT1 mcrB9999 rpsL150* (Str^r)	Laboratory collection
B462	DH2 *lacI*^{q} *gyrA462 zei*::Tn*10*	15
CSH50λ *sfiA*::*lacZ*	*ara* Δ(*lac-pro*) *strA thi sfiA*::*lacZ*	15
SG22622	MC4100 *cpsB*::*lacZ ara malP*::*lacI*^{q}	77
SG22622 *gyrA462*	SG22622 containing the *gyrA462* $CcdB_F$ resistance mutation	77
ω3326	DH5α/*pUC18*::phd_{SI}	This work
ω3379	ω3326/*pSU18T*::doc_{SI}	This work
ω3761	ω3730/*pSU18*::doc_{P1}	This work
ω3338	β2163/*pUC18*::phd_{SI}	This work
ω3481	ω3338/*pSU18T*::doc_{SI}	This work
ωB217	ω3326/*pSU18T*	This work
CSH50-1	CSH50/*pJL-OPphd-doc*$_{SI}$	This work
CSH50-2	CSH50/*pJL-OPphd-doc*$_{P1}$	This work
CSH50-3	CSH50/*pJL-OPccd*$_F$	This work
CSH50-4	CSH50/*pJL-OPccd*$_{Vfi}$	15

cases when brought to the first position(s) in the array (for a review, see reference 21). Cassette recombination is triggered in times of stress, as integron integrase expression is commonly controlled by the SOS response (24, 25), but also when horizontal gene exchanges occur (26, 27). Thus, between two episodes of stress, the cassette arrays stay steady, and one considers that the selective pressure exerted on distal silent cassettes is low if not absent. Several studies have shown that the *Vibrio cholerae* SI cassette array is a highly variable region that could be used to discriminate different *V. cholerae* serogroups and even isolates of the same serogroup. Using primers designed to anneal to the highly conserved *V. cholerae* cassette *attC* sites, historically named VCR (Vibrio cholerae repeats [28]), several teams have proposed PCR-based typing applications on SI unique variability (29–33). The *V. cholerae* N16961 SI carries 13 cassettes encoding putative type II TA systems (5, 17). The TA genes carried in 9 of these 13 cassettes are carried in the opposite orientation to that of other genes in the cassettes, preventing TA expression from the promoter located in *attI* sites that directs cassette gene expression (34). However, these TA genes are among the rare cassettes that can carry their own promoter, as there is sufficient space within the cassette boundaries to carry expression signals in the region located 5′ of the TA genes. The fact that these cassettes are most likely expressed lead us to propose that they could play a stabilization role by preventing cassette loss through homologous recombination between identical *attC* sites or between copies of repeated identical cassettes (17, 18). Data on the *higBA* and *parDE V. cholerae* TA cassettes gave further support to this role (35–37).

In this work, we describe the characterization of two SI cassettes encoding putative SI TA systems. The first is the $phd\text{-}doc_{SI}$ cassette, which we identified through the analysis of the *V. cholerae* N16961 genome sequence (17). We first developed a simple SI PCR typing strategy, based on the previously published SI/VCR typing applications mentioned above, to determine both the SI *intIA* proximal and distal cassettes in the SI cassette array. We applied this to the characterization of SI variation in 36 strains from the Pasteur Institute collection (CIP) of different origins, isolation dates, and serogroups (15 were from non-O1/non-O139 or unknown serogroup, while the others were of serogroup O1 or O139). This strategy allowed the definition of 15 SI types defined by the sequence of the first cassette(s) in the SI, which are supported by whole-genome sequencing data obtained for different *V. cholerae* strains. We then determined the distribution of the $phd\text{-}doc_{SI}$ cassette among these different *V. cholerae* strains, as well as in 5 *Vibrio metschnikovii* strains, where this cassette is also found (17). We show that this cassette, which is in position 72 in the *V. cholerae* N16961 SI array, is expressed and encodes a functional TA system that does not regulate its own expression. We further establish that the SI Phd (Phd_{SI}) can prevent Doc_{P1} toxicity and conversely that Phd_{P1} can prevent the Doc_{SI} deleterious effect.

The second cassette that we characterized is the *ccd* cassette from *V. fischeri* SI (17). As for the *phd-doc* cassette, we demonstrate that this cassette encodes a functional TA system with an active promoter and is expressed when in its original SI context. We show that the $CcdB_{Vfi}$ toxin targets DNA gyrase, and we found that the CcdA-B_{Vfi} complex regulates the cassette expression, in a fashion similar to the ccd_F operon of conjugative plasmid F. We also tested its functional interactions with the ccd_F system. We also tested both $phd\text{-}doc_{SI}$ and ccd_{Vfi} for their aptitude to mediate post-segregational killing (PSK) when carried on an unstable vector. Altogether, our results clearly support a role of SI stabilization but also suggest that these cassettes can play a protective role against incoming MGE to a certain extent.

MATERIALS AND METHODS

Bacterial strains and growth conditions. The *Escherichia coli* strains used in this work are described in Table 1, *Vibrio cholerae* strains in Table 2, and *Vibrio metschnikovii* and *Vibrio fischeri* strains in Table 3. *E. coli*, *V. cholerae*, and *V. metschnikovii* strains were grown in Luria-Bertani (LB) or on LB agar at 37°C and Ceria 132 synthetic medium supplemented with 0.1% Casamino Acids (CMM [38]). *V. fischeri* strains were grown in marine broth (MB) or marine agar (MA) at 30°C. When appropriate, media were supplemented with chloramphenicol (Cm; 5 mg/ml for *V. cholerae* or 25 mg/ml for *E. coli*), spectinomycin (Sp; 100 μg/ml for *V. cholerae* or 50 μg/ml for *E. coli*), kanamycin (Km; 25 μg/ml for *E. coli* and *V. cholerae* or 75 μg/ml for *V. fischeri*), and ampicillin (Ap; 100 μg/ml).

TABLE 2 *Vibrio cholerae* strains included in this study[a]

SI subtype[b]	Strain	Isolation yr	Source	Origin	Serogroup	Biotype
I	N16961	**1975**	**CIP**	**Bangladesh**	**O1 Inaba**	**Eltor**
II	**MJ-1236**	**1994**		**Clinical, Bangladesh**	O1 Inaba	Matlab variant of Eltor
	63.32	1961	CIP	Hong Kong	O1	Eltor
	68.10	1968	CIP	Vietnam	O1	ND
	254	1991	C. A. Salles	Human, Brazil	O1	ND
	104151	1992	CIP	Human, Bangladesh	O139	ND
	104152	1993	CIP	Human, Bangladesh	O139	ND
	1024	1961	J.-M. Fournier	Philippines	ND	ND
III	**M66-2**	**1937**		**Indonesia**		
	66.2	1966	CIP	Indonesia	O1	Eltor
	182	1983	C. A. Salles	Australia	O1	ND
	1023	1937	J.-M. Fournier	Indonesia	ND	ND
IV	**12129**	**1985**		**Water, Australia**	**O1 Inaba**	**Eltor**
	A256	1953	CIP		O1 Inaba	Eltor
V	**V52**	**1968**		**Clinical, Sudan**	**O37**	
	335	1965	C.A. Salles	Czechoslovakia	Non-O1	ND
VI	723	1954	C.A. Salles	Food, Thailand	Non-O1/O139	ND
VII	63.40	1935	CIP		Non-O1, non-O139	Nanking
VIII	63.41	1935	CIP		Non-O1, non-O139	Eltor
IX	104153	1989	CIP	Water, Bangladesh	Non-O1, non-O139	ND
X	104154	1987	CIP	Water, Bangladesh	Non-O1, non-O139	ND
XI	151	1986	C. A. Salles	Mexico	Non-O1	ND
XII	**VL426**	**?**		**Water, Maidstone, UK**	**Non-O1, non-O139**	**Albensis**
	69.41	1958	CIP	Fish, Germany	Non-O1, non-O139	ND
XIII	**O395**	**1965**		**India**	**O1 Ogawa**	**Classical**
	569B	1940	J.-M. Fournier	Human, India	O1	ND
	62.14	1959	CIP	Thailand	O1	ND
	62.15	1959	CIP	Thailand	O1	ND
	62.16	1959	CIP	Thailand	O1	ND
	A269	1943	CIP		O1	ND
	55.91	1953	CIP		O1	ND
	1143	1959	J.-M. Fournier	India	ND	ND
	1144	1947	J.-M. Fournier	Egypt	ND	ND
	1145	1953	J.-M. Fournier	India	ND	ND
XIV	ME11672	1993	M. Gallas	Water, Argentina	Non-O1, non-O139	ND
XV	BA5	1993	M. Gallas	Water, Argentina	Non-O1, non-O139	ND

[a] Genome sequences are accessible for strains in boldface type. ND, not determined.
[b] See the text for definition of SI subtypes; sequences are available at the following GenBank accession numbers: I, KC691400; II, KC691401; III, KC683366; IV, KC683367; V, KC691402; VI, KC683368; VII, KC691399; VIII, KC691403; IX, KC691404; X, KC683369; XI, KC683370; XII, KC691405; XIII, KC691406, XIV, KC683371; XV, KC683372.

PCR procedures. Error-free PCRs were performed in 50-μl mixtures by using *Pfu* DNA polymerase (Promega) following the manufacturer's instructions. Other PCRs were performed in 50-μl mixtures by using PCR Reddy mix (Abgène, United Kingdom) following the manufacturer's instructions. Primers were obtained from Sigma (Evry, France) and are listed in Table 4. The conditions used for amplification were as follows: 94°C for 5 min, followed by 30 cycles of 94°C for 30 s, 60°C for 30 s, and 72°C for 60s. The sequence of each cloned PCR product used in the dif-

TABLE 3 *Vibrio metschnikovii* and *Vibrio fischeri* strains used in this study

Species	Strain	Isolation yr	Source	Origin	*phd-doc*$_{SI}$	*ccdAB*$_{Vfi}$
V. metschnikovii	A267	1888	CIP	Poultry	+	−
	69.14T	1922	CIP	Diseased fowl	+	−
	69.15	1954	CIP	Unknown	+	−
	8050	1980	CIP	Human urine, Nevers, France	+	−
	104262	1977	CIP	Cooked cockles, Maidston, UK	+	−
V. fischeri	103206T (ATCC 7744)	1889	CIP	Unknown	−	+
	ES114	1990	P. Dunlap	Light organ symbiont of the squid *Euprymna scolopes* (78)	−	−

TABLE 4 Oligonucleotides used in this study

Primer name	Sequence (5′-3′)	Restriction site
I4	GCGAACACTTAACAAAAACTGGG	
VCR1	GTCCCTCT-TGAGGCGTTTGTTA	
VCR2	GCCCCTTAGGCGGGCGTTA	
829-2	TTCCACTGCGCCATTTACTGA	
829-7	TCTGTCACTACAGGTTTGCC	
32-2	GCATTCTTTGCGTCACACTATGGC	
VPD1	CGGGATCCCGTTTGTTTAGAGAGCTGAATTTTGTTCT	BamHI
VPD2	GGAATTCCTTATGTTT TTTATCACGTTTTG	EcoRI
VP1	GGATCCTCATTACATATCAGCCAATTTAGTGAATGT	BamHI
VP2	GGAATTCCAGGAGTGATTATGAATCGAAAAGTTGAAGC	EcoRI
VPQF	TGTAGCCGTTGTTCTTGACG	
VPQR	GAACGAGCATCTTCGTTTGA	
VD1	CGGGATCCCGTTAGAGAGCTGAATTTTGTTCTTTTGC	BamHI
VD2	GGAATTCCGGAGATCCTAATGGATATCATCTGTTTTCCTTTTGA	EcoRI
VD3	GCTCTAGAGCTTAGAGAGCTGAATTTTGTTCTTTTGC	XbaI
pVPI	CGCGGATCCTTTCGATTCATATCACACCTACTATCAATAAAGGTTAGGCCG	BamHI
pVP2	GGGAATTCTAGATTAACCCCTTAGGCGGGCGTTATGTTTTTTATCACGTTTTGGGGCTATAATCGGCCTAACCT	EcoRI
PP.D1	CGGGATCCATCTACTCCGCAGAACCATACA	BamHI
PP.D2	GGAATTCCGTTTATGCAATCCATTAACTTCCGT	EcoRI
PP1	CGGGATCCTATCGGTTAACCAGTTCCTTGTTG	BamHI
PP2	GGAATTCATGAGGCATATATCACCGGAAGAA	EcoRI
PDP1	GCTCTAGAGCCTACTCCGCAGAACCATACA	XbaI
5CcdAVfRI	TTGTGAATTCTATGAGAAATCAATATAATACACAAGCGG	EcoRI
3CcdAVfPI	AGTCTCTGCAGTTAAAATACTCGGTATGA	PstI
5CcdBVfXb	TCTAGAAGGAGGTTTAAATGTCTCAATTTACGCTATATAAAAACAAAGAT	XbaI
3CcdBVfPI	AGTCTCTGCAGTTTA AATGCCAGTGAT	PstI
5O/P-ccdVf	CTGCAGATGCATTTGTTAAATG	PstI
3O/P-ccdVf	AAGCTTACCGCTTGTGTATTATATTG	HindIII
pSFN1-1	AACTGCAGAACCAATGCATTGGCGCGCTATCGCTTGTCGGCC	PstI
pSFN1-2	CCCAAGCTTAAGAGCAGGGCTTTATATAGGACG	HindIII
ccdVf1	GGAATTCCGAGGTATTTTTAAATGTCTCAATTTACGCTAT	EcoRI
ccdVf2	CGGGATCCTTAAATGCCAGTGATTAAAAATCCC	BamHI
proVch-for	CCCCCTGCAGCCCTTAGGCGGGCGTTATGTTTTTTATCACGTTTTGGGGCTATAATCGGCCTAACCTTTATTGA TAGTAGGTGTGATAAGCTTCCCC	PstI- HindIII
proVch-rev	GGGGAAGCTTATCACACCTACTATCAATAAAGGTTAGGCCGATTATAGCCCCAAAACGTGATAAAAAACA TAAC GCCCGCCTAAGGGCTGCAGGGGG	PstI- HindIII
proP1-for	GGGGAAGCTTAAACACCTCGTGTACTCGTTATGTGTACACAATTATAAACTTCACAGGCATAAAGCACCA GCAC TGCAGGGGG	PstI- HindIII
proP1-rev	CCCCCTGCAGTGCTGGTGCTTTATGCCTGTGAAGTTTATAATTGTGTACACATAACGAGTACACGAGGTGTTTA AGCTTCCCC	PstI- HindIII
Oli94	GGAATTCCATGCATTTGTTAAATG	EcoRI
Oli95	GGATCCTTAAATGCCAGTGATTAA	BamHI
Oli96	CTGCAGATGCATTTGTTAAATG	PstI
Oli97	AAGCTTACCGCTTGTGTATTATATT	EcoRI
5′phd-docVch	CCCCGAATTCCCCTTAGGCGGGCGTTAT	EcoRI
3′phd-docVch	CCCCGAATTCCCCTTAGGCGGGCGTTAT	BamHI
5′phd-docP1′	CCCCGAATTCTGCTGGTGCTTTATGCCTGT	EcoRI
3″phd-docP1′	CCCCGGATCCATCTACTCCGCAGAACCATA	BamHI
MRV	AGCGGATAACAATTTCACACAGGA	
MFD	CGCCAGGGTTTTCCCAGTCACGAC	
16SQF	TCAGCTCGTGTTGTGAAATG	
16SQR	GTAAGGGCCATGATGACTTG	

ferent constructions described in this work was verified. Sequencing was performed by MWG-Biotech AG (Ebersberg, Germany) and with ABI Prism Applied Biosystem 3100 Genetic Analyzer.

Characterization of the *V. cholerae intIA* proximal and distal parts. The *intIA* proximal SI cassette(s) was amplified with primers I4 and VCR1 (39) and the distal SI cassette region with primers VCR2 (22) and either 829-2 or 32-2, using the *V. cholerae* strains listed in Table 2 as the templates. The PCR products were digested with HincII and inserted into pUC18 or pNot218, digested by the same enzyme, and sequenced with MRV and MFD primers.

TABLE 5 Plasmids used and constructed

Plasmid	Properties	Reference or source
pNOT218	oriColE1, Ap^r	79
pSU18	oriP15A, Cm^r	80
pSU18T	pSU18 $oriT_{RP4}$	42
pSU38	oriP15A, Km^r	80
pSU38T	pSU38 $oriT_{RP4}$	This work
pUC18	oriColE1, Ap^r	81
pUC19	oriColE1, Ap^r	81
pCR-XL-TOPO	oriColE1, Ap^r	82
pBAD33	oriP15A, Cm^r, P_{BAD}::MCS	83
pBAD43	oripSC101, Sp^r, P_{BAD}::MCS	83
p3326	pUC18::phd_{SI}	This work
p3730	pUC18::phd_{P1}	This work
p3178	pSU18::doc_{SI}	This work
p3974	pBAD43::doc_{SI}	This work
p4009	pBAD43::doc_{P1}	This work
p1400	pTZ19R::$ccdAB_{Vfi}$	17
pJL207	p15A, Cm^r, *lacZ*	84
p3481	pSU18T::doc_{SI}	This work
pSFN1	pB1067	46
pSU38TgV	pSU38T-$oriV_{pSFn1}$	This work
p9939	pSU38TgV::$ccdB_{Vfi}$	This work
p3610	pSU18T::$ccdB_{Vfi}$	This work
pBAD-*ccd*BF	pBAD33::$ccdB_F$	15
pBAD-*ccd*BVfi	pBAD33::$ccdB_{Vfi}$	This work
pKK223-3	ColE1, Ap^r, P_{TAC} promoter	85
pKK-*ccd*AVfi	*pKK223-3*::$ccdA_{Vfi}$	This work
pJL-OP*ccd*Vfi	pJL207::*O/P* $ccdB_{Vfi}$::*lacZ*	This work
pJL-OP*ccd*F	pULB2006	45
pJL-OP*phd-doc*$_{SI}$	pJL207::*O/P* phd_{SI}::*lacZ*	This work
pJL-OP*phd-doc*$_{P1}$	pJL207::*O/P* phd_{P1}::*lacZ*	This work
pMLO59	pGB2 ts derivative, Sp^r	15
pMLO-phd-doc$_{SI}$	pMLO59::*phd-doc*$_{SI}$	This work
pMLO-phd-doc$_{P1}$	pMLO59::*phd-doc*$_{P1}$	This work
pMLO-ccd$_{Vfi}$	pMLO59::ccd_{Vfi}	This work
pMLO-ccdF	pULB2710	46

RNA preparation and RT-PCR. Total RNA was purified from LB cultures harvested in the middle and at the end of the exponential phase as previously described (40). Reverse transcriptase PCR (RT-PCR) was performed on 500 ng *V. cholerae* N16961 total RNA with VP1 and VP2 primers (Table 4) using the Access RT-PCR system (Promega) with or without AMV reverse transcriptase. Real-time quantitative RT-PCRs were performed and analyzed as previously described (41), except that a 2-min preincubation at 90°C was replaced by 5 min at 80°C. The expression level of tested genes was normalized using the 16S rRNA gene of *V. cholerae* (primers 16SQF and 16SQR; Table 4). The experiments were repeated twice independently.

Plasmids. Plasmids used in this study are listed in Table 5.

Plasmid constructions. All plasmids and intermediate constructs were sequenced.

(i) Plasmids expressing phd_{SI} or phd_{P1}. *phd* genes were amplified from *V. cholerae* N16961 and P1 phage chromosomal DNA, using primers VP1 and VP2 or PP1 and PP2. PCR products were digested with EcoRI and BamHI and inserted into pUC18, digested by the same enzymes.

(ii) Plasmids expressing doc_{SI} or doc_{P1}. *doc* genes were amplified from *V. cholerae* N16961 and P1 phage chromosomal DNA, using the primers VD2 and VD3 or PD2 and PD3. PCR products were digested with EcoRI and XbaI and inserted into pBAD43, digested by the same enzymes. These plasmids, pBAD43::doc_{SI} and pBAD43::doc_{P1}, do not express *doc* in the presence of 1% glucose but do express *doc* in the presence of 0.2% arabinose. pSU18::doc_{SI} was constructed by cloning of the doc_{SI} gene after amplification using primers VD2 and VD1 for cloning of the product into pSU18 using EcoRI and BamHI. The ligation mix was transformed into a DH5α strain containing plasmid p3326, which expresses phd_{SI} to prevent Doc toxicity and is compatible with pSU18.

(iii) Plasmids expressing $ccdB_F$ and $ccdB_{Vfi}$. The expression plasmids are isogenic, i.e., all the open reading frames (ORFs) were cloned using the same restriction sites in the expression vectors and all the regulatory sequences added by PCR. The Shine-Dalgarno box (SD) and the sequence between the SD and the ATG of the ORFs were identical. pBAD-$ccdB_F$ plasmid has been described previously (15). pBAD-$ccdB_{Vfi}$ plasmid was constructed as follows: the *ccdB* gene from *V. fischeri*, $ccdB_{Vfi}$, was amplified by PCR using p1400 (17) as the template and the primers 5CcdBVfXb and 3CcdBVfPI. The PCR fragment XbaI site was blunted with the Klenow enzyme and then restricted by PstI. The resulting fragment was inserted into pUC19 digested by SmaI and PstI. The resulting plasmid was then digested by XbaI and PstI. The fragment containing $ccdB_{Vfi}$ was inserted into pBAD33 digested by the same enzymes. The ligation mixture was transformed in B462.

For pKK-$ccdA_{Vfi}$ plasmid, the *ccdA* gene from *V. fischeri*, $ccdA_{Vfi}$, was amplified by PCR using p1400 (17) as the template and the primers 5CcdAVfRI and 3CcdAVfPI. The PCR product was cloned into the TOPO-XL vector (Invitrogen). The resulting plasmid was then digested by EcoRI and PstI. The fragment containing $ccdA_{Vfi}$ was inserted into pKK223-3 using the same enzymes.

(iv) Conjugative plasmids expressing doc_{SI}, $ccdB_{Vfi}$, or $ccdB_F$. An expression vector able to be transferred by conjugation and to replicate in *V. fischeri* was constructed starting from the p15A derivative pSU38, by cloning the oriTRP4 as described previously for pSU18T (42). As neither ColE1 nor p15A derivatives are stably replicated in *V. fischeri*, we added in pSU38T, a fragment containing the replication origin of the *Vibrio nigripulchritudo* plasmid pSFn1 (43), also called pB1067 (44). This plasmid is the paradigm of a plasmid group commonly found in *Vibrio* species and that has been shown to replicate in all *Vibrio* species, including *V. fischeri*, when tested (44). $OriV_{pSFn1}$ was amplified from pSFn1 using primers pSFN1-1 and pSFN1-2. The PCR product was digested with PstI and HindIII and inserted into pSU38T (p3337) digested by the same enzyme to give pSU38TgV (p9887). The $ccdB_{Vfi}$ gene was amplified from *V. fischeri* CIP103206T, using primers Ccdvf1 and Ccdvf2. PCR products were digested with EcoRI and BamHI and inserted into pSU38TgV, digested by the same enzymes, and transformed in B462, leading to plasmid p9939 (pSU38TgV::$ccdB_{Vfi}$).

(v) Promoter activity reporter plasmids. To construct the pJL-OP-*phd-doc*$_{SI}$ plasmid, 2 complementary oligonucleotides, proVch-for and proVch-rev, encompassing the operator/promoter region of the *phd-doc*$_{SI}$ operon were synthesized. Annealing of these primers (1 μg each) was performed by slow cooling at room temperature after heating. The double-strand product was then restricted by HindIII and PstI and cloned in the pJL207 vector restricted by the same restriction enzymes. Recombinant clones were screened on minimal medium containing X-Gal (5-bromo-4-chloro-3-indolyl-β-D-galactopyranoside).

To construct the pJL-OP*phd-doc*$_{P1}$ plasmid, a similar procedure was followed with primers proP1-for and proP1-rev.

To construct the pJL-OPccd_{Vfi} plasmid, the operator/promoter region of the ccd_{Vfi} operon was amplified by PCR using the p1400 plasmid (17) as a template and the primers Oli96 and Oli97. The PCR product was cloned into the pCR-XL-TOPO vector (Invitrogen). A resulting plasmid with the insert in the proper orientation was then digested by HindIII and PstI (sites from the TOPO-XL vector). The fragment containing the operator/promoter region of the ccd_{Vfi} operon was inserted into pJL207 digested with the same enzymes. Recombinant clones were screened on MacConkey lactose medium.

Plasmid pJL-OPccd_F has been described in reference 45 under the designation pULB2006.

(vi) Postsegregational killing plasmids. To construct the pMLO-*phd-doc*$_{SI}$ plasmid, the *phd-doc*$_{SI}$ operon was amplified by PCR using primers 5′phd-doc$_{Vch}$ and 3′phd-doc$_{Vch}$. The PCR product was cloned into the pMLO59 plasmid digested by EcoRI and BamHI.

To construct the pMLO-*phd-doc*$_{P1}$ plasmid, the *phd-doc*$_{P1}$ operon was amplified by PCR using a P1*vir* as a template and primers 5′phd-doc$_{P1}$ and 3′phd-doc$_{P1}$. The PCR product was cloned into the pCR-XL-TOPO vector. The resulting plasmid was then digested by EcoRI and BamHI. The fragment containing the *phd-doc*$_{P1}$ operon was inserted into pMLO59 digested with the same enzymes.

To construct the pMLO-*ccd*$_{Vfi}$ plasmid, the *ccd*$_{Vfi}$ operon was amplified by PCR using the p1400 plasmid (17) as a template and primers Oli94 and Oli95.

The PCR product was cloned into the TopoXL vector. The resulting plasmid was then digested by EcoRI and BamHI. The fragment containing the *ccd*$_{Vfi}$ operon was inserted into pMLO59 digested with the same enzymes.

Plasmid pMLO-*ccd*$_{F}$ has been described previously under the designation pULB2710 (46).

Conjugations. Conjugations were performed as previously described (47) and repeated at least three times. Briefly, overnight cultures of donor and recipient cells were diluted 100-fold in LB and grown to an optical density (OD) of ~0.5. Donor and recipient cells were then mixed in a 1:1 ratio on 0.45-μm conjugation filters on LB plates preheated at 37°C when the recipient was *V. cholerae* or at 30°C when it was *V. fischeri*. After overnight incubation at 37°C (*V. cholerae*) or 30°C (*V. fischeri*), the filter was suspended in 5 ml LB, and dilutions were plated on selective plates to determine (i) the number of conjugants and (ii) the total number of recipients. Plasmid presence in transconjugant was checked by PCR with primers pSFN1-1 and pSFN1-2 on 8 randomly chosen clones. The new broad-host-range mobilizable vector pSU38TgV, constructed for this study (see above), was transferred from *E. coli* strain ω3480 to *V. fischeri* strain CIP 103206T at $1.6 \times 10^{-4} \pm 0.5 \times 10^{-4}$ and to strain ES114 at $3.1 \times 10^{-4} \pm 0.5 \times 10^{-4}$.

Toxicity and antitoxicity assays. Strains carrying the toxin-expressing plasmids and/or the antitoxin-expressing plasmid were grown overnight at 37°C in CCM supplemented with glucose (0.4%) and the appropriate antibiotics. Overnight cultures were diluted in the same medium to an OD at 600 nm (OD_{600}) of ~0.01 and grown at 37°C to an OD_{600} of ~0.1 to 0.2. The cultures were centrifuged at 4,000 rpm for 10 min at room temperature. The bacterial pellets were resuspended in CCM, prewarmed at 37°C, and supplemented with glycerol (0.4%) and the appropriate antibiotics. Arabinose was then added (0.25% or 1%), and the cultures were grown at 37°C. Samples were removed at indicated time points, diluted in $MgSO_4$ (10 mM), and plated on CCM plates supplemented with glucose (0.4%) and the appropriate antibiotics. Plates were incubated overnight at 37°C.

Postsegregational killing assay. CSH50λ*sfiA*::*lacZ* strains containing the pMLO59 vector and its derivatives were grown overnight at 30°C in LB containing Sp (100 μg/ml). Overnight cultures were centrifuged at 4,000 rpm for 10 min at room temperature and suspended in LB. Cultures were then diluted 400-fold in LB at 42°C. Cultures were diluted every 50 min to maintain an OD_{600} of 0.1 to 0.2. Samples were removed at indicated times, diluted in $MgSO_4$ (10 mM), and plated on LB plates and on LB plates supplemented with Sp. Plates were incubated overnight at 30°C. Numbers of CFU/ml on LB Sp plates at 42°C were similar for each pMLO59 derivative, indicating that these plasmids were lost at the same frequency (not shown).

Promoter activity assay. CSH50/pJL-OP*ccd*$_{F}$, CSH50/pJL-OP*ccd*$_{Vfi}$, CSH50/pJL-OP*phd-doc*$_{P1}$, and CSH50/pJL-OP*phd-doc*$_{P1}$ containing the pMLO59 vector or its derivatives were grown at 30°C in LB containing Cm (20 μg/ml) and Sp (100 μg/ml) to an OD_{600} of 0.3. Samples were removed, and β-galactosidase assays were performed as described in reference 48. Promoter activity was calculated as the ratio of β-galactosidase activity in the absence of the TA systems to that in the presence of the corresponding TA systems.

RESULTS

Determination of the different SI subtypes carried in *V. cholerae* strains. Several studies have shown that the SI cassette array was highly remodeled between different *V. cholerae* serogroups, and even among isolates of the same serogroup. Several laboratories have proposed PCR-based typing applications on this unique variability (29–33). In order to get a better view of SI variability and, in parallel, of the *phd-doc*$_{SI}$ cassette distribution, we designed a simple PCR strategy (see Fig. S1 in the supplemental material) to characterize the *intIA* proximal cassette(s), the distal cassettes content of the SI, and the *phd-doc*$_{SI}$ cassette presence and context among 36 *V. cholerae* strains (Table 2). Using a primer specific for the *intIA* gene (I4) and the primer VCR1 (39), we were able to amplify the very first cassette(s) present in all the strains tested. Indeed, VCR1 hybridizes with one of the two most conserved parts of the VCR, the *V. cholerae*-specific *attC* site, and thus allows the amplification of most *V. cholerae* cassettes as previously shown (39). The different amplicons were sequenced and allowed the retrieval of 15 different types of identical first-cassette arrangement and sequences (Fig. 1). In parallel, we performed a second PCR assay in order to characterize the distal part of the SI. For each strain, two PCRs were performed, which both used primer VCR2 (22), which hybridizes with the other most conserved sequence of the VCR and is oriented inversely to VCR1, and either primer 829-2 or 32-2, which are specific to the first gene downstream of the SI cassette array VCA0510 in N16961 or of Orf-32 in 569B (49). In all strains, one of these two PCRs gave rise to an amplification product, which after sequencing allowed the definition of 9 different distal parts (Fig. 1). As several *V. cholerae* strains' genome sequences became available during the course of this study, we also analyzed their *intIA* proximal SI cassette structure, determined to which of the 15 types they belong, and included this information in Table 2.

***phd-doc*$_{SI}$ cassette occurrence in the different *V. cholerae* and *V. metschnikovii* strains.** We further established the distribution of the *phd-doc*$_{SI}$ cassette in these different *V. cholerae* SI subtypes and in the five different *V. metschnikovii* strains available at the Pasteur Institute collection (CIP) (Table 3). We performed two PCRs for each of the SI subtype strains, the first with primer PD1, a primer located upstream of the *phd* gene and oriented toward the inside of the cassette, and VCR1, and the second with PD1 and PD2, a primer located inside *doc* oriented toward the 5′ end of the gene. We found that only strains from subtypes VI, VII, and XII did not carry the *phd-doc*$_{SI}$ cassette (not shown), while strains from the other 12 *V. cholerae* subtypes carried this cassette. In subtypes I, II, III, V, and XIII, the *phd-doc*$_{SI}$ cassette context was identical to the one of N16961 (Fig. 2), where a cassette that has lost most of its VCR site precedes it (17). We have been able to characterize the *phd-doc*$_{SI}$ cassette context in three other SI subtypes (Fig. 2). In strain 104153 (subtype IX), the cassette is preceded by a cassette with a canonical *attC* site, also found in *V. vulnificus*, while in strain A256 (subtype IV) the cassette contains an IS*1004* copy inserted 21 bp upstream of the *phd* gene (Fig. 2). In the latter, analysis of the sequence also revealed that the *doc* gene carried a mutation in codon 40, and that led us to test its functionality (see below). Finally, we found that in subtype XI, the *phd-doc*$_{SI}$ cassette was the last of the SI cassette array. Moreover, this

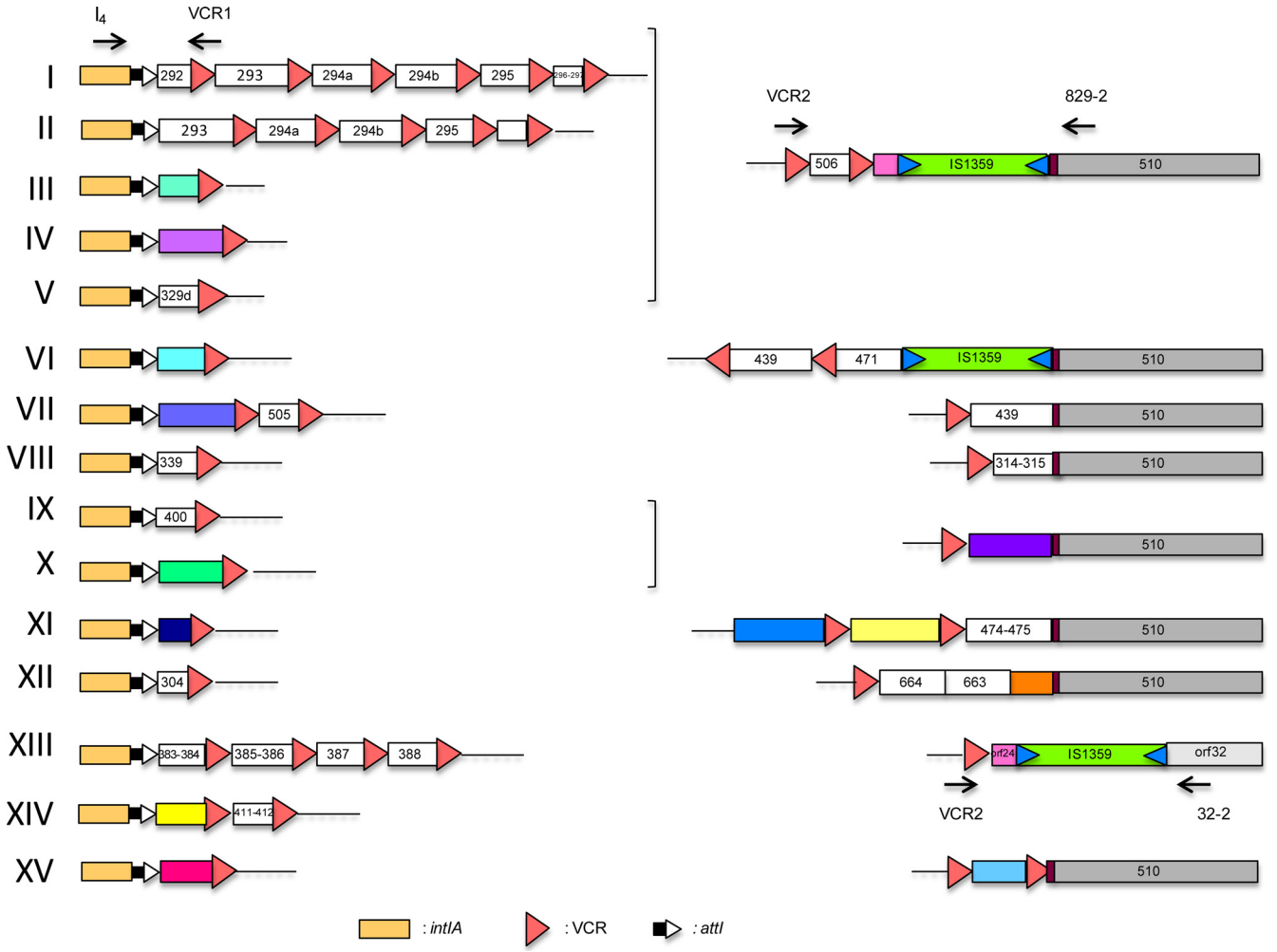

FIG 1 *Vibrio cholerae* superintegron subtypes. Each of the 15 subtypes is defined by a superintegron having both a specific *intIA* proximal cassette(s) and a distal end of the cassette array. Subtypes are numbered in Roman numerals; *intIA*, VCR, and *attI* symbols are described in the figure. ORFs carried in cassettes that are found in the N16961 reference genome sequence are identified as white boxes, and the corresponding VCA0XXX identification is given by the last 3 digits; when the carried cassettes are not found in the N16961 genome, they are symbolized with colored boxes. The primers used for the subtype determination (see the text), their orientation, and their locations are indicated by black arrows. Insertion sequences (IS) are symbolized by boxes carrying two triangles pointing inside the box.

cassette was now immobilized due to the loss of its associated VCR (Fig. 2). All *V. metschnikovii* strains were found to carry the cassette (Table 3). We found that strains 69.14T and 69.15 carried the *phd-doc*$_{SI}$ cassette downstream of the same cassette (Orf253 to -255) in strain A267, where we previously described this TA cassette (17), while its context was different, but unknown, in the 2 other strains (data not shown).

Functional characterization of the *phd-doc*$_{SI}$ system in *E. coli*. In order to establish if the *phd-doc*$_{SI}$-encoded proteins were functional, we tested it in *E. coli*, which does not naturally carry a *phd-doc* TA system. After PCR amplification from *V. cholerae* N16961 genomic DNA with appropriate primers, we cloned the *phd*$_{SI}$ gene, which encodes the putative antidote to the Doc$_{SI}$ toxin in pUC18 (Ap^r), under the control of the P$_{lac}$ promoter, leading to plasmid pUC18::*phd* (p3326). In parallel, we amplified the *doc*$_{SI}$ gene and cloned it in a compatible plasmid, pSU18T, which carries a chloramphenicol resistance marker (Cm^r), and transformed strain ω3326 (DH5α pUC18::*phd*). Transformation of DH5α with the same ligation mix did not produce any Cm^r clones (not shown). One ω3326 transformant, carrying both compatible plasmids carrying *doc*$_{SI}$ and *phd*$_{SI}$, was named ω3379. In parallel, ω3326 was also transformed with the empty pSU18T, giving rise to ωB217. The plasmids carried in both strains, pUC18::*phd* and pSU18T::*doc* in ω3379 and pUC18::*phd* and pSU18T in ωB217, were extracted. These plasmid mixes were then digested by endonuclease NdeI, which specifically cleaves pUC18::*phd* but neither pSU18T nor pSU18T::*doc*. These NdeI-treated samples, which contain only propagative pSU18T derivatives, were then used to transform either DH5α or ω3326 (DH5 α/pUC18::*phd*). Both samples gave approximately the same number of Cm^r clones in ω3326, while the Cm^r clone frequency in DH5α dropped to 1% after transformation with the ω3379 sample (pSU18T::*doc* plus linearized pUC18::*phd*) compared to what is obtained with the ωB217 sample (pSU18T plus linearized pUC18::*phd*) (Table 6). Replica plating of those DH5α Cm^r clones obtained after transformation with ω3379 NdeI-treated sample on LB Ap plates,

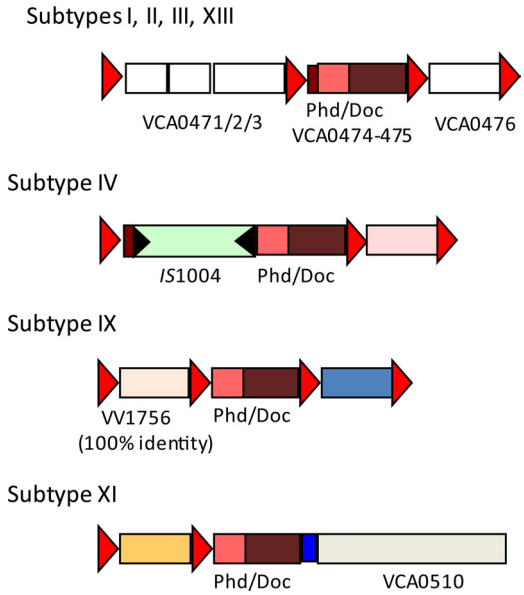

FIG 2 Genetic context of the *phd-doc* cassette in different *V. cholerae* superintegron subtypes. Subtypes are identified by their Roman numeral (Fig. 1). ORFs carried in cassettes that are found in the N16961 reference genome sequence are identified as white boxes, and the corresponding VCA0XXX identification is given by the last 3 digits; when the carried cassettes are not found in the N16961 genome, they are symbolized with colored boxes. Red triangles correspond to the VCRs of the different cassettes, and black triangles symbolize the inverted repeats (IRs) of IS*1004*.

showed that all Cm^r clones were also Ap^r. The lack of ApS Cm^r clones demonstrates the functionality of both genes in *E. coli*: doc_{SI}, encoding the toxin, and phd_{SI}, encoding its antidote.

The *phd-doc*$_{SI}$ cassette is functional and expressed from the *V. cholerae* superintegron. In order to establish the functionality of this TA module in *V. cholerae*, we used a strategy similar to the one described above, using conjugation to deliver the doc_{SI} gene in a strain carrying (N16961, subtype I) or lacking (CIP 63-40, subtype VII) the *phd-doc*$_{SI}$ cassette. We used two different donor strains, both carrying a nonmobilizable pUC18::phd_{SI} and either the compatible and mobilizable Cm^r plasmid pSU18T::doc_{SI} or an empty pSU18T. We then made a conjugation between these two donors and either N16961 or CIP 63-40 as the recipient and selected for Cm^r transconjugants. Under these conditions, with N16961, we obtained Cm^r transconjugants for both the empty pSU18-oriT and its doc_{SI} derivative, at the same frequency (10^{-2}). This shows that the phd_{SI} gene is expressed from its cassette context in N16961 and could prevent Doc_{SI} toxicity. With CIP 63-40, Cm^r transconjugants were obtained at the same frequency as in N16961 with the empty pSU18T, while with pSU18T::doc_{SI}, Cm^r clones were only obtained at a frequency of 10^{-6}. This difference suggested that Doc_{SI} was toxic in strain CIP 63-40. To further understand the origin of the few Cm^r clones in strain CIP 63-40 after transfer of the doc_{SI} plasmid, we replicated these clones on Ap plates and found that a fraction of them were Ap^r (data not shown). We then analyzed the plasmid content of a sample of the Ap^s and Ap^r transconjugants and found that Ap^r clones all carried cointegrates of pSU18T::doc_{SI} and pUC18::phd_{SI}, while the Ap^s clones carried a pSU18T::doc_{SI} containing a deletion covering most of the doc_{SI} gene, likely due to a replication slippage between two 11-bp-long repeats (not shown), inactivating its product. On the other hand, when we extracted the plasmids carried by the Cm^r clones obtained in N16961, the pSU18T::doc_{SI} did not show any modification and were found to still be toxic when transformed in *E. coli*.

In order to formally demonstrate the expression of *phd-doc* cassette, we performed a semiquantitative RT-PCR, with or without AMV reverse transcriptase, and found a single band only after reverse transcription (see Fig. S2 in the supplemental material), demonstrating its efficient transcription. Furthermore, expression of the *phd-doc* operon was analyzed by real-time quantitative RT-PCR on total RNA extracted from cells in mid-log or early stationary phases, and a 3-fold-higher expression of the cassette was observed in exponential growth than in stationary phase. These results demonstrate that the *phd-doc*$_{SI}$ cassette is expressed and functional in *V. cholerae*, Doc_{SI} being toxic and Phd_{SI} able to prevent its deleterious activity.

In strain A256, in which the *phd-doc*$_{SI}$ cassette is flanked by an IS*1004*, inserted 21 bp upstream of *phd*, analysis of the cassette sequence also revealed a mutation in codon 40 of the *doc* gene (CGA→TGA), leading to a premature stop. We checked that this mutation impaired the toxicity of the encoded Doc_{SIA256}, by transformation of *E. coli* with a plasmid expressing doc_{SIA256} in the absence of phd_{SI} in the recipient. We obtained transformants at similar rates with either the $pDoc_{SIA256}$ or the empty vector, showing that this mutation (R40*) inactivates Doc. We also tested if the IS*1004* insertion modifies phd_{SIA256} in the A256 SI context. In order to do that, we cotransformed strain A256 with pSU18::doc_{SI} (Cm^r) and pUC18::phd_{SI} (Ap^r), selected Cm^r transformants, and tested if they were also Ap^r. We found that all Cm^r clones were also Ap^r, showing that the phd_{SIA256} expression in the A256 SI context was extinct.

The *phd-doc* systems of phage P1 and *V. cholerae* are able to cross talk. The hypothesis that chromosomal TA could also play a role in the protection against incoming mobile elements, such as plasmids, interleukin-converting enzymes (ICEs), or lysogenic phages, implies that chromosomal systems should be able to counteract the TA systems brought by the invading element. As the Doc superfamily appears to be widespread in bacteria both on chromosomes and on plasmids (7), we tested the cross-interactions between the *phd-doc*$_{SI}$ of the vibrio superintegron and the canonical *phd-doc*$_{P1}$ of the P1 phage in *E. coli*. The two Doc proteins show 32% identity, while the two Phd proteins are less related (17% identity) and do not hit each other by BLASTP (see Fig. S3 in the supplemental material). The two *phd* genes were cloned in pUC18 under the P_{LAC} promoter, while the two *doc* genes were cloned in pBAD43, a low-copy-number SpR plasmid, under the P_{BAD} promoter. The two pBAD43::*doc* plasmids could be main-

TABLE 6 Demonstration of the functionality of Doc_{SI}/Phd_{SI} functionality as a toxin-antitoxin couple

DNA	Frequency[a] for CMR transformants coupled with:	
	DH5α	DH5α(pUC18::*phd*)
ωB217 DNA (pSU18T + linearized pUC18::*phd*)	$(1.12 \pm 0.3) \times 10^4$	$(3.8 \pm 0.3) \times 10^4$
ω3379 DNA (pSU18T::*doc* + linearized pUC18::*phd*)	$(2.7 \pm 0.2) \times 10^2$	$(1.9 \pm 0.3) \times 10^4$

[a] Normalized for 1 μg of NdeI-treated plasmid mix.

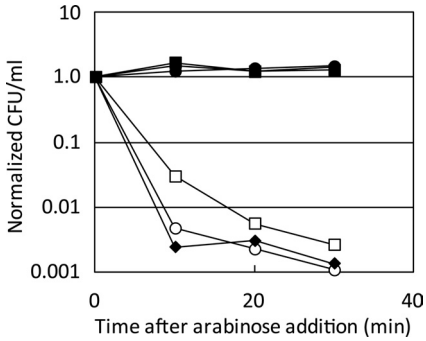

FIG 3 Interactions between the ccd_{Vfi} and ccd_F systems. SG22622/pKK223-3/pBAD-$ccdB_F$ (open square), SG22622/pKK223-3/pBAD-$ccdB_{Vfi}$ (open circle), SG22622/pKK-$ccdA_F$/pBAD-$ccdB_F$ (filled square), SG22622/pKK-$ccdA_{Vfi}$/pBAD-$ccdB_{Vfi}$ (filled circle), SG22622/pKK-$ccdA_F$/pBAD-$ccdB_{Vfi}$ (filled triangle), and SG22622/pKK-$ccdA_{Vfi}$/pBAD-$ccdB_F$ (filled diamond) were grown as described in Materials and Methods. After addition of 1% arabinose, serial dilutions of the cultures were plated without arabinose and incubated overnight at 37°C. The number of CFU per ml at each time point was normalized to that of time zero (just before arabinose addition) for each strain. This experiment was performed at least in duplicate.

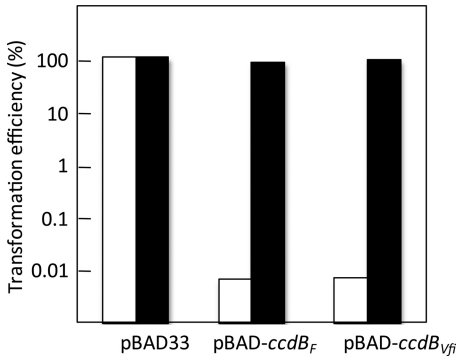

FIG 4 The $CcdB_{Vfi}$ toxin targets the DNA-gyrase. SG22622 (white bars) and SG22622*gyrA462* (black bars) were transformed with the control vector pBAD33 or the pBAD-$ccdB_F$ and pBAD-$ccdB_{Vfi}$ plasmids as indicated. Transformation mixtures were plated onto LB plates without arabinose or with 1% arabinose. The efficiency of transformation for each plasmid is the ratio of the number of transformants obtained on 1% arabinose plates to the number of transformants on plates without arabinose. This experiment was performed at least in triplicate.

tained in *E. coli* only in the presence of 1% glucose, while transfer to LB plus 0.2% arabinose killed the cells. We then transformed each of these two strains independently with either the pUC18::phd_{P1} or the pUC18::phd_{SI} and selected transformants in parallel on LB Sp Ap plus arabinose or plus glucose. We obtained the same number of transformants on all media, demonstrating that the two systems were able to interact and prevent the toxicity of the noncognate TA toxin.

The *V. fischeri* SI ccd_{Vfi} system is a toxin-antitoxin gene pair and is expressed from the *V. fischeri* superintegron. We had previously obtained indirect evidence of the $CcdB_{Vfi}$ toxic activity (17). To demonstrate the functionality of the two components, we used a strategy similar to the one used for $phd\text{-}doc_{SI}$ and for another *ccd* homologous system (15). The $ccdB_{vfi}$ gene was cloned in the pBAD33 vector (P_{BAD} promoter) and the $ccdA_{vfi}$ gene in the compatible pKK223-3 vector (P_{TAC} promoter). *E. coli* was first transformed by the pKK223-3 vector or its derivative carrying the $ccdA_{Vfi}$ gene. These strains were subsequently transformed with the pBAD33 vector or the pBAD33 plasmid carrying the $ccdB_{Vfi}$ gene. Transformation mixtures were plated on LB plates containing the appropriate antibiotics in the absence of inducer. The transformation efficiency for each plasmid was comparable to that of the pBAD33 control vector in each strain (data not shown).

The toxic activity of the toxin and the ability of its antitoxin to counteract its toxic activity were assayed in liquid cultures (Fig. 3). Production of the $CcdB_{Vfi}$ protein resulted in a dramatic loss of viability after 10 min of induction. Viability was not affected in the presence of its antitoxin, $CcdA_{Vfi}$. These results show that the *V. fischeri* SI ccd_{Vfi} system is a toxin-antitoxin gene pair.

To determine whether the $CcdB_{Vfi}$ toxin targets the DNA gyrase as shown for the $CcdB_F$ toxin (50), we transformed the pBAD-$ccdB_{Vfi}$ and pBAD-$ccdB_F$ plasmids in SG22622 and in the isogenic strain carrying the $CcdB_F$-resistant mutation *gyrA462* (strain SG22622 *gyrA462*). Figure 4 shows that the relative transformation efficiency for the pBAD-$ccdB_F$ and pBAD-$ccdB_{Vfi}$ plasmids in the wild-type strain was very low in the presence of 1% arabinose ($<10^{-4}$), while it was comparable to that of the vector in SG22622 *gyrA462* (about 10^0) (Fig. 4). Thus, the *gyrA462* mutation enables transformation of pBAD-$ccdB_F$, a pBAD33 derivative expressing $ccdB_F$ (15), as well as of the pBAD-$ccdB_{Vfi}$ plasmid upon induction, showing that the $CcdB_{Vfi}$ toxins also target the DNA gyrase.

We originally identified the ccd_{Vfi} cassette through the partial characterization of the integron cassette array found in the *V. fischeri* type strain (CIP 103206T) (17). Analysis of the genome of *V. fischeri* ES114, the *Euprymna scolopes* squid light organ symbiont, which was determined in 2005 (51), revealed the absence of the ccd_{Vfi} cassette in this strain. In order to determine if this TA module was expressed in its original genetic context, we introduced by conjugation a plasmid able to replicate in *V. fischeri* and expressing $ccdB_{Vfi}$, pSU38TgV::*ccd*BVfi (p9939), in both *V. fischeri* strains CIP 103206T and ES114, and selected transconjugants on Km, the resistance brought by the plasmid marker. Km^r clones carrying plasmid p9939 were obtained in *V. fischeri* CIP 103206T only at a frequency ($1.7 \times 10^{-4} \pm 0.54 \times 10^{-4}$) similar to the one obtained for the empty pSU38TgV vector ($1.6 \times 10^{-4} \pm 0.5 \times 10^{-4}$). Strain ES114 Km^r clones were obtained only at low frequency (10^{-6}) and likely corresponded to spontaneous Km^r mutants, as these clones were all found to lack p9939 by PCR. In order to check that CIP 103206T Km^r transconjugants were carrying p9939 with a functional $ccdB_{Vfi}$, we purified the plasmid from several clones and transformed *E. coli* strains B462, a CcdB-resistant strain, and DH5α. We obtained transformants in B462 only, demonstrating that $ccdB_{Vfi}$ was still functional and expressed in these plasmids. Altogether, these results strongly support that ccd_{Vfi} is expressed from the SI context.

Ability of the $CcdA_F$ and $CcdA_{Vfi}$ antitoxins to counteract their noncognate toxins. It is not clear whether the ccd_{Vfi} system coexists with the ccd_F system, although plasmid conjugation between *E. coli* and *Vibrio fischeri* has already been demonstrated in a laboratory context (52). However, it is unlikely that F can replicate in *V. fischeri*, as it cannot be maintained in *V. cholerae* (53). We tested the functional interactions between the antitoxins and the toxins of the ccd_F and the ccd_{Vfi} systems. As for Phd-Doc, here too the two toxins are more related to each other than the two antitoxins, with 41% identity between the CcdBs and 22% identity between the CcdAs (see Fig. S4 in the supplemental material). The ability of the different antitoxins to counteract the toxic activity of

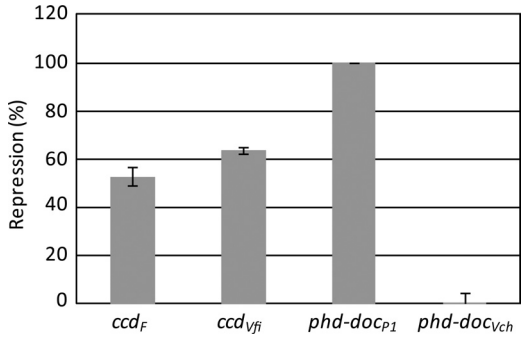

FIG 5 Autoregulation of the ccd_{Vfi} and $phd\text{-}doc_{SI}$ systems. Strain CSH50 containing the different promoter-*lacZ* fusions and the pMLO59 vector or its derivatives carrying the corresponding TA systems were grown at 30°C, and promoter activity was measured at mid-log phase. The graph represents the percentage of repression of each promoter in the presence of the corresponding TA system. The experiments were performed in triplicate.

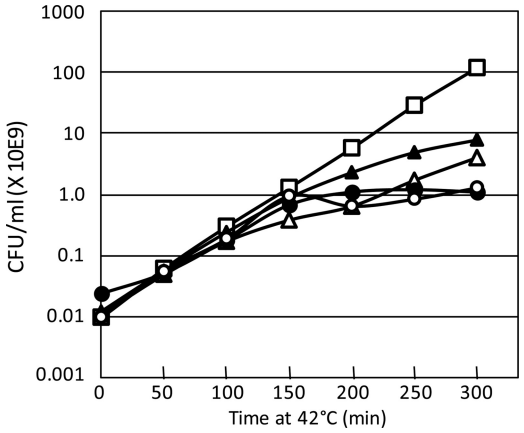

FIG 6 Ability of the ccd_{Vfi} and $phd\text{-}doc_{SI}$ systems to mediate postsegregational killing. CSH50 λ*sfiA*::*lacZ* strains containing the pMLO59 vector (open square) and its derivative carrying the ccd_F (filled triangle), ccd_{Vfi} (open triangle), $phd\text{-}doc_{P1}$ (closed circle), or $phd\text{-}doc_{SI}$ (open circle) systems were grown at 30°C in LB as described in Materials and Methods. Cultures were sampled at the times indicated in the figure, and viability was measured (in CFU/ml). These experiments were performed in duplicate.

the different toxins was assayed in liquid cultures. Expression of $CcdB_F$ and $CcdB_{Vfi}$ toxins resulted in a dramatic loss of viability, while viability was restored by coexpression of $CcdA_F$ (Fig. 3). This shows that the $CcdA_F$ antitoxin is able to counteract the toxic activity of the SI cassette toxin as efficiently as its cognate toxin. However, expression of the $CcdA_{Vfi}$ antitoxin was not able to counteract $CcdB_F$ efficiently (Fig. 3).

Autoregulation of the ccd_{Vfi} and $phd\text{-}doc_{Vch}$ systems. The putative promoter regions of the ccd_{Vfi} and $phd\text{-}doc_{SI}$ systems were cloned in the pJL207 plasmid carrying a promoter-free *lacZ* gene in a fashion similar to what has been previously published for the ccd_F system (45) (see Materials and Methods). Interestingly, while the promoter activity of $phd\text{-}doc_{SI}$ was comparable to that of the P1 system, the activity of the ccd_{Vfi} was 3.4-fold higher than that of its F plasmid counterpart (data not shown). Figure 5 shows that the ccd_{Vfi} system is autoregulated, as expected, by the $CcdA_{Vfi}$ and $CcdB_{Vfi}$ proteins expressed in *trans*. The repression appears to be similar to that of the ccd_{Vfi} system (40 to 60% repression). For $phd\text{-}doc_{SI}$, we were unable to detect any repression, while repression of $phd\text{-}doc_{P1}$ was very efficient, being nearly complete.

Ability of the ccd_{Vfi} and $phd\text{-}doc_{Vch}$ systems to mediate postsegregational killing. The ccd_{Vfi} and $phd\text{-}doc_{SI}$ systems were cloned in a conditionally replicating (thermosensitive) plasmid, pGB2 (see Materials and Methods). Figure 6 shows that after 150 min of culture at 42°C, the ability of the strains carrying the four systems to form colonies decreased in comparison with that of the control strain. Efficiency levels of the $phd\text{-}doc_{SI}$ and $phd\text{-}doc_{P1}$ systems to mediate postsegregational killing (PSK) were comparable, and after 300 min at 42°C, more than 99% of the population was unable to form colonies. The ccd_{Vfi} system was slightly more efficient than ccd_F between 150 and 250 min at 42°C, but overall, at 300 min, the two were comparable.

Postsegregational killing relies on the Lon-dependent degradation of the $CcdA_F$ antitoxin (46). We therefore compared the postsegregational SOS induction mediated by the loss of the pMLO59-ccd_{Vfi} plasmid at 42°C in CSH50λ*sfiA*::*lacZ* and in CSH50 *lon*::Tn*10* λ*sfiA*::*lacZ* strains. Postsegregational SOS induction was completely abolished in the CSH50 *lon*::Tn*10* λ*sfiA*::*lacZ* strain (data not shown). This shows, though indirectly, that like the $CcdA_F$ antitoxin, $CcdA_{Vfi}$ is also a substrate of the Lon ATP-dependent protease.

DISCUSSION

In order to be able to couple the detection of the presence of $phd\text{-}doc_{SI}$ cassette with the variability of the SI cassette array, we devised a simple PCR-typing strategy, based on three sets of primers that allowed the determination of the variability in the *intIA* proximal and distal parts of the SI cassette array of *V. cholerae* strains and isolates. After sequencing the different PCR products corresponding to the *intIA* proximal SI cassette(s), we were able to define 15 SI subtypes from the 36 strains from the Pasteur Institute collection (CIP) of different origins, isolation dates, and serogroups (15 were from non-O1/non-O139 or unknown serogroup, while the others were of serogroup O1 or O139) (Table 2 and Fig. 1). Our results confirm the highly discriminative power of such SI-based typing (32), as O1 strains were distributed among 5 SI subtypes, though it cannot be substituted for serogroup typing, as SI subtype II gathers O1 and O139 strains. However, inside a given serogroup it can help to discriminate among different clones and be useful for epidemiological studies. It has been observed in the class 1 integron that cassette integration preferentially occurs at the *attI* site and leads to more variability in the first position than in remote positions (54). The fact that less variability is observed in the distal part of the SI than in the *attI* proximal part suggests that this is also likely true in the *V. cholerae* SI. Analysis of the $phd\text{-}doc_{SI}$ cassette presence in the 36 strains showed a perfect match between the subtyping and the presence or absence of this cassette, showing that loss of the cassette was coupled with reordering mediated by extensive cassette recombination. This cassette was absent in only 3 of the 15 SI subtypes, which are defined by only one strain (SI subtypes VI and VII; Table 2) or two strains (SI subtypes XII; Table 2). We also demonstrated the presence of this cassette in the six *V. metschnikovii* strains that we tested.

We functionally characterized this $phd\text{-}doc_{SI}$ cassette, as well as the ccd_{Vfi} cassette so far found only in *V. fischeri*. These two type II TA systems belong to the families that are the least represented among the SI TA cassettes, compared to *relBE* or *parDE*, for example (5). We demonstrated that the two cassettes encode functional proteins and carry their own active promoters. We further

showed that the two cassettes were efficiently expressed from their SI context, in *V. cholerae* N16961 for *phd-doc*$_{SI}$, and in *V. fischeri* CIP 103206T for *ccd*$_{Vfi}$. The *phd-doc*$_{SI}$ cassette is likely expressed in all *V. cholerae* and *V. metschnikovii* strains when present, with one notable exception in *V. cholerae* strain A256. Indeed, in this strain, we found that an IS*1004* insertion a few base pairs upstream of *phd* reduces its expression to a level that does not allow inhibition of Doc$_{SI}$ toxicity when expressed in *trans* from a p15A vector, while in the absence of IS*1004*, the Phd$_{SI}$ level of expression from the SI is sufficient to prevent the Doc$_{SI}$ toxicity when expressed from the plasmid. In addition, in this strain the *doc* toxin gene is inactivated by a premature stop codon, while the *phd* sequence is native.

There are only 2 other TA systems from the *phd-doc* family that have been characterized to a certain extent, one in the *Yersinia pestis* chromosome (55) and the original one, discovered in the phage P1 genome (56), which has been extensively studied. Doc$_{P1}$ has been shown to interact with the 30S ribosomal subunit, and its toxicity is the result of inhibition of translation elongation, possibly at the translocation step (57). The Doc$_{SI}$ toxin shares 30% identity to Doc$_{P1}$, while the Phd$_{SI}$ is only distantly related to Phd$_{P1}$ (17% identity), and they are even further less related to the *Y. pestis* proteins, 21% and <10%, respectively. However, BLASTP screening of databases with Phd$_{SI}$ as query detects 3 related proteins, which are parts of other putative *phd-doc* TAs, with an encoded Doc much more related to the SI TA than to the P1 one. Two are found in marine bacteria. The first is carried in the genome of *Desulfotalea psychrophila* LSv54 (accession number for Phd, YP065779-1, and for Doc, YP65772-1) (58), and its products share 66% and 85% identity to Phd$_{SI}$ and Doc$_{SI}$, respectively; however, both encoded proteins are truncated in their C-terminal part and are likely inactive. The second TA is carried in the large plasmid pSba102 found in *Shewanella baltica* OS155 (accession number for Phd, YP00104727-1, and for Doc, EHY 78006-1) (73% and 62% identity to Phd$_{SI}$ and Doc$_{SI}$, at the protein level). The third one is carried in the genome of the plant pathogen *Pseudomonas syringae* pv. mori str. 301020 (accession number for Phd, EGH24474-1, and for Doc, EGH24475-1) and shows 73 and 77% identities with Phd$_{SI}$ and Doc$_{SI}$, respectively. Analysis of the genetic contexts of these different *phd-doc* stystems does not reveal any cassette structural features. Interestingly, Docs are generally much more constrained, and BLASTP screening of databases with Doc$_{SI}$ is able to hit the Doc$_{P1}$ protein, while as mentioned above, Phd$_{SI}$ detects only three related proteins and not Phd$_{P1}$. The Phd$_{SI}$ and the Phd proteins encoded by both *S. baltica* and *P. syringae* are 56 amino acids (aa) long (the *D. psychrophila* LSv54 Phd protein is truncated at the C terminus and lacks 5 aa) and thus much shorter that the 73-aa-long Phd$_{P1}$. Interestingly, the alignment of these proteins suggests that the difference in size is due to an N-terminal truncation in Phd$_{SI}$ and its two related Phd (see Fig. S1 in the supplemental material). The crystal structure shows that Phd$_{P1}$ forms a heterotetrameric 2:2 complex with Doc$_{P1}$ (59). It has been shown for Phd$_{P1}$ that the C-terminal domain (residues 52 to 73) harbors the site of interaction with Doc$_{P1}$ and that this domain is sufficient to prevent Doc-mediated growth arrest (60). On the other hand, the N-terminal region (residues 1 to 51) of Phd$_{P1}$ corresponds to the dimerization/DNA-binding domain that has been shown to bind to the operator site of the *phd-doc*$_{P1}$ operon (60, 61) and to regulate the TA operon expression (62). Operator binding and repression of the *phd-doc*$_{P1}$ operon by Phd$_{P1}$ are enhanced by the presence of Doc$_{P1}$ in a cooperative manner (63, 64). Thus, the N-terminal truncation found in Phd$_{SI}$ may explain why there is no transcriptional autoregulation. The C-terminal part of the Phd$_{SI}$ is only poorly related to the one of Phd$_{P1}$, but several of the amino acids identified as important for the Phd$_{P1}$-Doc$_{P1}$ interaction through genetic or structural studies are conserved (59–61, 65, 66) (see Fig. S1 in the supplemental material). The demonstration we made that Phd$_{SI}$ can prevent the DocP1 toxicity and, vice versa, that Phd$_{P1}$ can prevent the Doc$_{SI}$ toxicity shows that the overall structure and biochemical properties of the interaction regions are conserved.

The characterization of the *ccd*$_{Vfi}$ system further confirmed that this operon encodes a functional TA system, which has the same characteristics as the *ccd*$_{F}$ system. We demonstrated here that even if only remotely related to the CcdB$_{F}$ (37% identity), CcdB$_{Vfi}$ targets DNA gyrase in a similar fashion, as inferred from the insensitivity of the *E. coli gyrA462* mutant toward the toxin activity, even if a recent structural study suggests that the CcdB$_{vfi}$ binding to GyrA involves slightly different interactions than those made by CcdB$_{F}$ (67). The three-dimensional (3D) structure of crystals of CcdB$_{Vfi}$ in complex with a GyrA fragment (GyrA14, amino acids 362 to 493) has been recently published (68), showing that CcdB$_{Vfi}$ and CcdB$_{F}$ recognize the same surface of DNA gyrase fragment (67). Furthermore, the key amino acids of the toxic active site of CcdB$_{F}$ that had been previously identified as glycine100 and isoleucine101 (69) are conserved in CcdB$_{Vfi}$ (see Fig. S2 in the supplemental material).

We obtained evidence that CcdA$_{Vfi}$ is degraded by the Lon protease pathway, similarly to what has been found for CcdA$_{F}$ and its homologue CcdA$_{O157}$ (15, 46). We found that the *ccd*$_{Vfi}$ system is at least as efficient to trigger postsegregational SOS induction as is the *ccd*$_{F}$ system (15) and as efficient to mediate plasmid stabilization. Finally, we found that the *ccd*$_{Vfi}$ operon expression is tightly autoregulated by the CcdA$_{Vfi}$ and CcdB$_{Vfi}$ proteins, similarly to what has been observed in the *ccd*$_{F}$ system.

Chromosomal TA systems have been proposed to stabilize chromosomal regions by preventing accidental deletions (17), especially when located in unstable segments such as mobile genetic elements (MGE) (18, 19). The study made by Rowe-Magnus and collaborators on the RelBE1 and ParDE1 cassettes carried in the *Vibrio vulnificus* SI has substantiated this role. Indeed, they showed that both systems were expressed *in vivo* and that the activity of the proteins encoded in the two TAs counterbalanced the extent of deletions catalyzed by the class 1 integron integrase IntI1 (18). Furthermore, the presence of TA gene cassettes in SIs did not preclude integrase-mediated microevolution from occurring; *en masse* gene cassette loss was suppressed, but the exchange of individual cassettes continued. The net effect was stabilization of SI gene cassette arrays in the absence of selection, and this activity may in part explain why gene cassettes coding for TA systems are common in large SIs but are absent from smaller SIs, like the resistance integrons (21). The studies of the *V. cholerae* cassettes encoding TA systems of the HigBA and ParDE families also support this role (35–37, 70). Here, we demonstrated that two other TA cassettes, carried in the SI of different *Vibrio* species, are also expressed in their original context, suggesting that all the SI TA cassettes share this stabilization role. It would be interesting to determine if, when multiple TA cassettes from the same functional family are found in the same SI, all are expressed and if they all evolved in such a way that they do not cross-interact, as has been

already shown for the three ParDE and the two HigBA cassettes of the *V. cholerae* N16961 SI (35, 37).

These chromosomal TA systems can also potentially protect their host genome from colonization by an incoming mobile element or a plasmid carrying a TA from the same functional family, by allowing its harmless loss through the neutralization of the invading toxin by the chromosomal antitoxin (15, 17, 71). In order to substantiate this hypothesis, we tested the functional interactions between these two SI TA systems and those carried in MGE. These two systems are among the least represented, and unfortunately we did not find related systems carried in the MGE characterized in these species, or in close relatives. However, we tested the interaction of the *phd-doc*$_{SI}$ with the phage P1 system, and the *ccdAB*$_{Vfi}$ with the plasmid F homologous system. In the Phd-Doc cross talk experiment, we found that both Doc toxins could be antagonized by both antitoxins, showing that if a P1 phage was able to somehow infect *V. cholerae* its lysogenic state would be destabilized by the products expressed from the SI *phd-doc* cassette. As mentioned above, we identified *in silico* a closely related and likely functional *phd-doc* operon in the unpublished sequence of a large plasmid, pSba102, from a marine bacterium, *Shewanella baltica* OS155 (accession number, NC_009036). As *V. metschnikovii* and *V. cholerae* are also marine bacteria, it is possible that such a plasmid or a related one can be exchanged among these species, and it would have been interesting to establish the cross talks between these two *phd-doc* systems. In the case of the *ccd* systems, we obtained different results in similar cross talk experiments between the *V. fischeri* and plasmid F systems. Indeed, we have shown that the CcdA$_{Vfi}$ antitoxin is unable to counteract the toxic activity of CcdB$_F$ while the CcdA$_F$ antitoxin is able to counteract the CcdB$_{Vfi}$ toxin (Fig. 3). We had previously observed similar one-way interaction between the *ccd*$_F$ system and the chromosomal system found in *E. coli* O157:H7 (15), while Matsuba and colleagues had made a similar observation for the PemK toxin of the *pem* (*parD*) TA system located on the R100 (R1) plasmid of *E. coli* and the two antitoxins of its chromosomal homologues, which are unable to counteract the toxicity of the plasmid-encoded toxin (72), except when mutated (71). YefM-YoeB homologues carried either on plasmids or on chromosomes have also been found to poorly cross talk, at most (73, 74). Thus, it appears that the plasmidic systems are "dominant" over their chromosomal homologues in many cases. One may imagine that evolution has selected that type of hierarchy between homologous TA systems. Chromosomal TA systems like those found in the SI cassettes might thus also serve as exclusion systems to protect bacteria from being loaded with an excess of exogenous DNA-carrying related TA systems (plasmids, transposons, and phages), a function related to the one of restriction-modification systems (see reference 75). Our results and previous observations described above suggest that selective pressure on plasmidic TA systems to evade chromosomal TA cross-interaction is extremely strong. However, some chromosomal systems are able to mediate antiaddiction and protect the cell against PSK (16). It is very unlikely that F can replicate in *V. fischeri*, as we found that if F can be conjugated in vibrios, such as *V. cholerae*, it cannot replicate in this species (53). It is also very unlikely that phage P1 can infect *Vibrio* species. However, as these two TAs are embedded in integron cassettes, they may also exist in different hosts, where F or P1 can be more likely encountered.

From the structural point of view, the fact that the Phd$_{SI}$ proteins counteract the Doc$_{P1}$ proteins and vice versa is surprising, especially as the CcdA$_{Vfi}$ proteins do not counteract the CcdB$_F$ proteins. Indeed Phd$_{SI}$ and Phd$_{P1}$ are only remotely related, both in size and in sequence, and the two Doc proteins share only 30% identity, while the two CcdB proteins share a higher identity (37%), as do the two CcdA proteins, which share 20% identity over the whole length of the proteins. These cross talk pattern differences may reflect intrinsic properties of the two different TA systems or a selective constraint linked to the fact that they naturally compete in common hosts. In this line, it would be very interesting to determine the interactions between the PhD-Doc of pSab102 and those encoded in the *Vibrio* SI, to see if, while more closely related among them than with the P1 proteins, they evolved to prevent cross-interactions.

ACKNOWLEDGMENTS

We thank Jason Bland for helpful reading of the manuscript.

Work in the Mazel laboratory is funded by the Institut Pasteur, the Centre National de la Recherche Scientifique (CNRS-UMR 3525), the French National Research Agency (ANR-08-MIE-016), the French Government's Investissement d'Avenir program, Laboratoire d'Excellence "Integrative Biology of Emerging Infectious Diseases" (grant no. ANR-10-LABX-62-IBEID) and the European Union Seventh Framework Programme (FP7-HEALTH-2011-single-stage) "Evolution and Transfer of Antibiotic Resistance" (EvoTAR), and the Fondation pour la Recherche Médicale (équipe FRM 2007). Work in the laboratory of L.V.M. is supported by the Fonds de la Recherche (FRSM-3.4530.04), Fondation Van Buuren, and Fonds Jean Brachet. N.I. was supported by a Franco-Pakistani doctoral fellowship.

REFERENCES

1. **Gerdes K, Christensen SK, Lobner-Olesen A.** 2005. Prokaryotic toxin-antitoxin stress response loci. Nat. Rev. Microbiol. **3**:371–382.
2. **Van Melderen L, Saavedra De Bast M.** 2009. Bacterial toxin-antitoxin systems: more than selfish entities? PLoS Genet. **5**:e1000437. doi:10.1371/journal.pgen.1000437.
3. **Yamaguchi Y, Park JH, Inouye M.** 2011. Toxin-antitoxin systems in bacteria and archaea. Annu. Rev. Genet. **45**:61–79.
4. **Fineran PC, Blower TR, Foulds IJ, Humphreys DP, Lilley KS, Salmond GP.** 2009. The phage abortive infection system, ToxIN, functions as a protein-RNA toxin-antitoxin pair. Proc. Natl. Acad. Sci. U. S. A. **106**:894–899.
5. **Pandey DP, Gerdes K.** 2005. Toxin-antitoxin loci are highly abundant in free-living but lost from host-associated prokaryotes. Nucleic Acids Res. **33**:966–976.
6. **Guglielmini J, Szpirer C, Milinkovitch MC.** 2008. Automated discovery and phylogenetic analysis of new toxin-antitoxin systems. BMC Microbiol. **8**:104. doi:10.1186/1471-2180-8-104.
7. **Leplae R.** 2011. Diversity of bacterial type II toxin-antitoxin systems: a comprehensive search and functional analysis of novel families. Nucleic Acids Res. **39**:5513–5525.
8. **Ramage HR, Connolly LE, Cox JS.** 2009. Comprehensive functional analysis of Mycobacterium tuberculosis toxin-antitoxin systems: implications for pathogenesis, stress responses, and evolution. PLoS Genet. **5**:e1000767. doi:10.1371/journal.pgen.1000767.
9. **Engelberg-Kulka H, Amitai S, Kolodkin-Gal I, Hazan R.** 2006. Bacterial programmed cell death and multicellular behavior in bacteria. PLoS Genet. **2**:e135. doi:10.1371/journal.pgen.0020135.
10. **Van Melderen L.** 2010. Toxin-antitoxin systems: why so many, what for? Curr. Opin. Microbiol. **13**:781–785.
11. **Christensen SK, Pedersen K, Hansen FG, Gerdes K.** 2003. Toxin-antitoxin loci as stress-response-elements: ChpAK/MazF and ChpBK cleave translated RNAs and are counteracted by tmRNA. J. Mol. Biol. **332**:809–819.
12. **Keren I, Shah D, Spoering A, Kaldalu N, Lewis K.** 2004. Specialized persister cells and the mechanism of multidrug tolerance in Escherichia coli. J. Bacteriol. **186**:8172–8180.

13. **Lewis K.** 2010. Persister cells. Annu. Rev. Microbiol. **64**:357–372.
14. **Nariya H, Inouye M.** 2008. MazF, an mRNA interferase, mediates programmed cell death during multicellular Myxococcus development. Cell **132**:55–66.
15. **Wilbaux M, Mine N, Guerout AM, Mazel D, Van Melderen L.** 2007. Functional interactions between coexisting toxin-antitoxin systems of the ccd family in Escherichia coli O157:H7. J. Bacteriol. **189**:2712–2719.
16. **Saavedra De Bast M, Mine N, Van Melderen L.** 2008. Chromosomal toxin-antitoxin systems may act as antiaddiction modules. J. Bacteriol. **190**:4603–4609.
17. **Rowe-Magnus DA, Guerout AM, Biskri L, Bouige P, Mazel D.** 2003. Comparative analysis of superintegrons: engineering extensive genetic diversity in the Vibrionaceae. Genome Res. **13**:428–442.
18. **Szekeres S, Dauti M, Wilde C, Mazel D, Rowe-Magnus DA.** 2007. Chromosomal toxin-antitoxin loci can diminish large-scale genome reductions in the absence of selection. Mol. Microbiol. **63**:1588–1605.
19. **Wozniak RA, Waldor MK.** 2009. A toxin-antitoxin system promotes the maintenance of an integrative conjugative element. PLoS Genet. **5**:e1000439. doi:10.1371/journal.pgen.1000439.
20. **Dziewit L, Jazurek M, Drewniak L, Baj J, Bartosik D.** 2007. The SXT conjugative element and linear prophage N15 encode toxin-antitoxin-stabilizing systems homologous to the tad-ata module of the Paracoccus aminophilus plasmid pAMI2. J. Bacteriol. **189**:1983–1997.
21. **Cambray G, Guerout AM, and Mazel D.** 2010. Integrons. Annu. Rev. Genet. **44**:141–166.
22. **Mazel D, Dychinco B, Webb VA, Davies J.** 1998. A distinctive class of integron in the *Vibrio cholerae* genome. Science **280**:605–608.
23. **Boucher Y, Labbate M, Koenig JE, Stokes HW.** 2007. Integrons: mobilizable platforms that promote genetic diversity in bacteria. Trends Microbiol. **15**:301–309.
24. **Guerin E, Cambray G, Sanchez-Alberola N, Campoy S, Erill I, Da Re S, Gonzalez-Zorn B, Barbe J, Ploy MC, Mazel D.** 2009. The SOS response controls integron recombination. Science **324**:1034.
25. **Cambray G, Sanchez-Alberola N, Campoy S, Guerin E, Da Re S, Gonzalez-Zorn B, Ploy MC, Barbe J, Mazel D, Erill I.** 2011. Prevalence of SOS-mediated control of integron integrase expression as an adaptive trait of chromosomal and mobile integrons. Mobile DNA **2**:6. doi:10.1186/1759-8753-2-6.
26. **Baharoglu Z, Mazel D.** 2011. Vibrio cholerae triggers SOS and mutagenesis in response to a wide range of antibiotics: a route towards multiresistance. Antimicrob. Agents Chemother. **55**:2438–2441.
27. **Baharoglu Z, Krin E, Mazel D.** 2012. Connecting environment and genome plasticity in the characterization of transformation-induced SOS regulation and carbon catabolite control of the Vibrio cholerae integron integrase. J. Bacteriol. **194**:1659–1667.
28. **Barker A, Clark CA, Manning PA.** 1994. Identification of VCR, a repeated sequence associated with a locus encoding a hemagglutinin in Vibrio cholerae O1. J. Bacteriol. **176**:5450–5458.
29. **Labbate M, Boucher Y, Joss MJ, Michael CA, Gillings MR, Stokes HW.** 2007. Use of chromosomal integron arrays as a phylogenetic typing system for Vibrio cholerae pandemic strains. Microbiology **153**:1488–1498.
30. **Feng L, Reeves PR, Lan R, Ren Y, Gao C, Zhou Z, Cheng J, Wang W, Wang J, Qian W, Li D, Wang L.** 2008. A recalibrated molecular clock and independent origins for the cholera pandemic clones. PLoS One **3**:e4053. doi:10.1371/journal.pone.0004053.
31. **Chun J, Grim CJ, Hasan NA, Lee JH, Choi SY, Haley BJ, Taviani E, Jeon YS, Kim DW, Brettin TS, Bruce DC, Challacombe JF, Detter JC, Han CS, Munk AC, Chertkov O, Meincke L, Saunders E, Walters RA, Huq A, Nair GB, Colwell RR.** 2009. Comparative genomics reveals mechanism for short-term and long-term clonal transitions in pandemic Vibrio cholerae. Proc. Natl. Acad. Sci. U. S. A. **106**:15442–15447.
32. **Chowdhury N, Asakura M, Neogi SB, Hinenoya A, Haldar S, Ramamurthy T, Sarkar BL, Faruque SM, Yamasaki S.** 2010. Development of simple and rapid PCR-fingerprinting methods for Vibrio cholerae on the basis of genetic diversity of the superintegron. J. Appl. Microbiol. **109**:304–312.
33. **Gao Y, Pang B, Wang HY, Zhou HJ, Cui ZG, Kan B.** 2011. Structural variation of the superintegron in the toxigenic Vibrio cholerae O1 El Tor. Biomed. Environ. Sci. **24**:579–592.
34. **Jove T, Da Re S, Denis F, Mazel D, Ploy MC.** 2010. Inverse correlation between promoter strength and excision activity in class 1 integrons. PLoS Genet. **6**:e1000793. doi:10.1371/journal.pgen.1000793.
35. **Christensen-Dalsgaard M, Gerdes K.** 2006. Two higBA loci in the Vibrio cholerae superintegron encode mRNA cleaving enzymes and can stabilize plasmids. Mol. Microbiol. **62**:397–411.
36. **Budde PP, Davis BM, Yuan J, Waldor MK.** 2007. Characterization of a higBA toxin-antitoxin locus in Vibrio cholerae. J. Bacteriol. **189**:491–500.
37. **Yuan J, Yamaichi Y, Waldor MK.** 2011. The three Vibrio cholerae chromosome II-encoded ParE toxins degrade chromosome I following loss of chromosome II. J. Bacteriol. **193**:611–619.
38. **Glansdorff N.** 1965. Topography of cotransducible arginine mutations in Escherichia coli K-12. Genetics **51**:167–179.
39. **Rowe-Magnus DA, Guerout AM, Mazel D.** 2002. Bacterial resistance evolution by recruitment of super-integron gene cassettes. Mol. Microbiol. **43**:1657–1669.
40. **Krin E, Danchin A, Soutourina O.** 2010. RcsB plays a central role in H-NS-dependent regulation of motility and acid stress resistance in Escherichia coli. Res. Microbiol. **161**:363–371.
41. **Krin E, Derzelle S, Bedard K, Adib-Conquy M, Turlin E, Lenormand P, Hullo MF, Bonne I, Chakroun N, Lacroix C, Danchin A.** 2008. Regulatory role of UvrY in adaptation of Photorhabdus luminescens growth inside the insect. Environ. Microbiol. **10**:1118–1134.
42. **Le Roux F, Binesse J, Saulnier D, Mazel D.** 2007. Construction of a Vibrio splendidus mutant lacking the metalloprotease gene vsm by use of a novel counterselectable suicide vector. Appl. Environ. Microbiol. **73**:777–784.
43. **Reynaud Y, Saulnier D, Mazel D, Goarant C, Le Roux F.** 2008. Correlation between detection of a plasmid and high-level virulence of Vibrio nigripulchritudo, a pathogen of the shrimp Litopenaeus stylirostris. Appl. Environ. Microbiol. **74**:3038–3047.
44. **Le Roux F, Davis BM, Waldor MK.** 2011. Conserved small RNAs govern replication and incompatibility of a diverse new plasmid family from marine bacteria. Nucleic Acids Res. **39**:1004–1013.
45. **Salmon MA, Van Melderen L, Bernard P, Couturier M.** 1994. The antidote and autoregulatory functions of the F plasmid CcdA protein: a genetic and biochemical survey. Mol. Gen. Genet. **244**:530–538.
46. **Van Melderen L, Bernard P, Couturier M.** 1994. Lon-dependent proteolysis of CcdA is the key control for activation of CcdB in plasmid-free segregant bacteria. Mol. Microbiol. **11**:1151–1157.
47. **Bouvier M, Demarre G, Mazel D.** 2005. Integron cassette insertion: a recombination process involving a folded single strand substrate. EMBO J. **24**:4356–4367.
48. **Zhou Y, Gottesman S.** 1998. Regulation of proteolysis of the stationary-phase sigma factor RpoS. J. Bacteriol. **180**:1154–1158.
49. **Clark CA, Purins L, Kaewrakon P, Focareta T, Manning PA.** 2000. The *Vibrio cholerae* O1 chromosomal integron. Microbiology **146**:2605–2612.
50. **Bernard P, Couturier M.** 1992. Cell killing by the F plasmid CcdB protein involves poisoning of DNA-topoisomerase II complexes. J. Mol. Biol. **226**:735–745.
51. **Ruby EG, Urbanowski M, Campbell J, Dunn A, Faini M, Gunsalus R, Lostroh P, Lupp C, McCann J, Millikan D, Schaefer A, Stabb E, Stevens A, Visick K, Whistler C, Greenberg EP.** 2005. Complete genome sequence of Vibrio fischeri: a symbiotic bacterium with pathogenic congeners. Proc. Natl. Acad. Sci. U. S. A. **102**:3004–3009.
52. **Dunlap PV, Kuo A.** 1992. Cell density-dependent modulation of the Vibrio fischeri luminescence system in the absence of autoinducer and LuxR protein. J. Bacteriol. **174**:2440–2448.
53. **Baharoglu Z, Bikard D, Mazel D.** 2010. Conjugative DNA transfer induces the bacterial SOS response and promotes antibiotic resistance development through integron activation. PLoS Genet. **6**:e1001165. doi:10.1371/journal.pgen.1001165.
54. **Collis CM, Recchia GD, Kim MJ, Stokes HW, Hall RM.** 2001. Efficiency of recombination reactions catalyzed by class 1 integron integrase IntI1. J. Bacteriol. **183**:2535–2542.
55. **Goulard C, Langrand S, Carniel E, Chauvaux S.** 2010. The Yersinia pestis chromosome encodes active addiction toxins. J. Bacteriol. **192**:3669–3677.
56. **Lehnherr H, Maguin E, Jafri S, Yarmolinsky MB.** 1993. Plasmid addiction genes of bacteriophage P1: doc, which causes cell death on curing of prophage, and phd, which prevents host death when prophage is retained. J. Mol. Biol. **233**:414–428.
57. **Liu M, Zhang Y, Inouye M, Woychik NA.** 2008. Bacterial addiction module toxin Doc inhibits translation elongation through its association with the 30S ribosomal subunit. Proc. Natl. Acad. Sci. U. S. A. **105**:5885–5890.
58. **Rabus R, Ruepp A, Frickey T, Rattei T, Fartmann B, Stark M, Bauer M,**

Zibat A, Lombardot T, Becker I, Amann J, Gellner K, Teeling H, Leuschner WD, Glockner FO, Lupas AN, Amann R, Klenk HP. 2004. The genome of Desulfotalea psychrophila, a sulfate-reducing bacterium from permanently cold Arctic sediments. Environ. Microbiol. **6**:887–902.

59. **Arbing MA, Handelman SK, Kuzin AP, Verdon G, Wang C, Su M, Rothenbacher FP, Abashidze M, Liu M, Hurley JM, Xiao R, Acton T, Inouye M, Montelione GT, Woychik NA, Hunt JF.** 2010. Crystal structures of Phd-Doc, HigA, and YeeU establish multiple evolutionary links between microbial growth-regulating toxin-antitoxin systems. Structure **18**:996–1010.
60. **Smith JA, Magnuson RD.** 2004. Modular organization of the Phd repressor/antitoxin protein. J. Bacteriol. **186**:2692–2698.
61. **McKinley JE, Magnuson RD.** 2005. Characterization of the Phd repressor-antitoxin boundary. J. Bacteriol. **187**:765–770.
62. **Gazit E, Sauer RT.** 1999. Stability and DNA binding of the Phd protein of the phage P1 plasmid addiction system. J. Biol. Chem. **274**:2652–2657.
63. **Magnuson R, Lehnherr H, Mukhopadhyay G, Yarmolinsky MB.** 1996. Autoregulation of the plasmid addiction operon of bacteriophage P1. J. Biol. Chem. **271**:18705–18710.
64. **Magnuson R, Yarmolinsky MB.** 1998. Corepression of the P1 addiction operon by Phd and Doc. J. Bacteriol. **180**:6342–6351.
65. **Garcia-Pino A, Christensen-Dalsgaard M, Wyns L, Yarmolinsky M, Magnuson RD, Gerdes K, Loris R.** 2008. Doc of prophage P1 is inhibited by its antitoxin partner Phd through fold complementation. J. Biol. Chem. **283**:30821–30827.
66. **Garcia-Pino A, Dao-Thi MH, Gazit E, Magnuson RD, Wyns L, Loris R.** 2008. Crystallization of Doc and the Phd-Doc toxin-antitoxin complex. Acta Crystallogr. Sect. F Struct. Biol. Cryst. Commun. **64**:1034–1038.
67. **De Jonge N, Simic M, Buts L, Haesaerts S, Roelants K, Garcia-Pino A, Sterckx Y, De Greve H, Lah J, Loris R.** 2012. Alternative interactions define gyrase specificity in the CcdB family. Mol. Microbiol. **84**:965–978.
68. **De Jonge N, Hohlweg W, Garcia-Pino A, Respondek M, Buts L, Haesaerts S, Lah J, Zangger K, Loris R.** 2010. Structural and thermodynamic characterization of Vibrio fischeri CcdB. J. Biol. Chem. **285**:5606–5613.
69. **Bahassi EM, Salmon MA, Van Melderen L, Bernard P, Couturier M.** 1995. F plasmid CcdB killer protein: ccdB gene mutants coding for noncytotoxic proteins which retain their regulatory functions. Mol. Microbiol. **15**:1031–1037.
70. **Yuan J, Sterckx Y, Mitchenall LA, Maxwell A, Loris R, Waldor MK.** 2010. Vibrio cholerae ParE2 poisons DNA gyrase via a mechanism distinct from other gyrase inhibitors. J. Biol. Chem. **285**:40397–40408.
71. **Santos Sierra S, Giraldo R, Diaz Orejas R.** 1998. Functional interactions between chpB and parD, two homologous conditional killer systems found in the Escherichia coli chromosome and in plasmid R1. FEMS Microbiol. Lett. **168**:51–58.
72. **Masuda Y, Miyakawa K, Nishimura Y, Ohtsubo E.** 1993. chpA and chpB, Escherichia coli chromosomal homologs of the pem locus responsible for stable maintenance of plasmid R100. J. Bacteriol. **175**:6850–6856.
73. **Grady R, Hayes F.** 2003. Axe-Txe, a broad-spectrum proteic toxin-antitoxin system specified by a multidrug-resistant, clinical isolate of Enterococcus faecium. Mol. Microbiol. **47**:1419–1432.
74. **Nieto C, Cherny I, Khoo SK, de Lacoba MG, Chan WT, Yeo CC, Gazit E, Espinosa M.** 2007. The yefM-yoeB toxin-antitoxin systems of Escherichia coli and Streptococcus pneumoniae: functional and structural correlation. J. Bacteriol. **189**:1266–1278.
75. **Kobayashi I.** 2001. Behavior of restriction-modification systems as selfish mobile elements and their impact on genome evolution. Nucleic Acids Res. **29**:3742–3756.
76. **Demarre G, Guerout AM, Matsumoto-Mashimo C, Rowe-Magnus DA, Marliere P, Mazel D.** 2005. A new family of mobilizable suicide plasmids based on broad host range R388 plasmid (IncW) and RP4 plasmid (IncPalpha) conjugative machineries and their cognate Escherichia coli host strains. Res. Microbiol. **156**:245–255.
77. **Allali N, Afif H, Couturier M, Van Melderen L.** 2002. The highly conserved TldD and TldE proteins of Escherichia coli are involved in microcin B17 processing and in CcdA degradation. J. Bacteriol. **184**:3224–3231.
78. **Boettcher KJ, Ruby EG.** 1990. Depressed light emission by symbiotic Vibrio fischeri of the sepiolid squid Euprymna scolopes. J. Bacteriol. **172**:3701–3706.
79. **Rowe-Magnus DA, Guerout A-M, Ploncard P, Dychinco B, Davies J, Mazel D.** 2001. The evolutionary history of chromosomal superintegrons provides an ancestry for multi-resistant integrons. Proc. Natl. Acad. Sci. U. S. A. **98**:652–657.
80. **Bartolome B, Jubete Y, Martinez E, de la Cruz F.** 1991. Construction and properties of a family of pACYC184-derived cloning vectors compatible with pBR322 and its derivatives. Gene **102**:75–78.
81. **Yanisch-Perron C, Vieira J, Messing J.** 1985. Improved M13 phage cloning vectors and host strains: nucleotide sequences of the M13mp18 and pUC19 vectors. Gene **33**:103–119.
82. **Bernard P, Gabant P, Bahassi EM, Couturier M.** 1994. Positive-selection vectors using the F plasmid ccdB killer gene. Gene **148**:71–74.
83. **Guzman LM, Belin D, Carson MJ, Beckwith J.** 1995. Tight regulation, modulation, and high-level expression by vectors containing the arabinose PBAD promoter. J. Bacteriol. **177**:4121–4130.
84. **Light J, Molin S.** 1982. The sites of action of the two copy number control functions of plasmid R1. Mol. Gen. Genet. **187**:486–493.
85. **Brosius J, Holy A.** 1984. Regulation of ribosomal RNA promoters with a synthetic lac operator. Proc. Natl. Acad. Sci. U. S. A. **81**:6929–6933.